Control of the Molecular Orientation of Membrane-Anchored Biomimetic Glycopolymers

Kamil Godula,[‡,¶,□] Marissa L. Umbel,[†] David Rabuka,[‡,●] Zsofia Botyanszki,[‡]
Carolyn R. Bertozzi,[‡,§,⊥,¶,□] and Raghuveer Parthasarathy*,[†]

*Department of Physics and Materials Science Institute, University of Oregon, Eugene, Oregon 97403.
Departments of Chemistry, Molecular and Cell Biology and Howard Hughes Medical Institute,
University of California, and Materials Sciences Division and The Molecular Foundry,
Lawrence Berkeley National Laboratory, Berkeley, California 94720*

Received April 23, 2009; E-mail: raghu@uoregon.edu

Abstract: Quantifying and controlling the orientation of surface-bound macromolecules is crucial to a wide range of processes in areas as diverse as biology, materials science, and nanotechnology. Methods capable of directing orientation, as well as an understanding of the underlying physical mechanisms are, however, lacking. In this paper, we describe experiments in which the conformations of structurally well-defined polymers anchored to fluid lipid membranes were probed using Fluorescence Interference Contrast Microscopy (FLIC), an optical technique that provides topographic information with few-nanometer precision. The novel rodlike polymers mimic the architecture of mucin glycoproteins and feature a phospholipid tail for membrane incorporation and a fluorescent optical probe for FLIC imaging situated at the opposite termini of the densely glycosylated polymeric backbones. We find that the orientation of the rigid, approximately 30 nm long glycopolymers depends profoundly on the properties of the optical reporter. Molecules terminated with Alexa Fluor 488 projected away from the lipid bilayer by 11 ± 1 nm, consistent with entropy-dominated sampling of the membrane-proximal space. Molecules terminated with Texas Red lie flat at the membrane (height, 0 ± 2 nm), implying that interactions between Texas Red and the bilayer dominate the polymers' free energy. These results demonstrate the design of macromolecules with specific orientational preferences, as well as nanometer-scale measurement of their orientation. Importantly, they reveal that seemingly minute changes in molecular structure, in this case fluorophores that comprise only 2% of the total molecular weight, can significantly alter the molecule's presentation to the surrounding environment.

Introduction

The orientation of surface-anchored macromolecules is a crucial determinant of function in contexts as diverse as molecular electronics,[1] DNA[2] and carbohydrate[3] microarrays, and membrane biophysics.[4] In the last category, interactions between cell surface proteins and their binding partners that can include soluble proteins, surface receptors of other cells, and the extracellular matrix require extension and projection away from the lipid bilayer and its proximate space. While the orientations of densely packed collections of molecules covalently linked to solid surfaces, for example alkanethiols on gold or chemically grafted DNA, can be largely determined by

the steric constraints of their packing arrangements, proteins at membranes are more sparsely linked to a two-dimensional fluid. The resulting freedom to explore their spatial and conformational neighborhood suggests that nontrivial mechanisms are required to control protein orientation. Such physical mechanisms, however, remain largely unexplored, subject so far to only a few controlled studies.[5−7] Elucidating principles of macromolecular orientation at membranes requires structurally well-defined biomimetic models as well as techniques capable of probing nanometer-scale topography.

Membrane mucins are a particularly important class of large cell-surface glycoproteins, involved in vital biological processes (e.g., cell migration, adhesion, and immunogenesis), as well as many pathological events (e.g., cancer metastasis).[8−10] The study of glycoprotein behavior at membranes poses considerable challenges due to the proteins' structural and compositional heterogeneity and nanoscale dimensions, far below the resolution limits of conventional optical microscopy. To address these challenges, we have developed a new class of uniform,

† University of Oregon.
‡ Department of Chemistry, University of California.
§ Department of Molecular and Cell Biology, University of California.
⊥ Howard Hughes Medical Institute, University of California.
¶ Materials Sciences Division, Lawrence Berkeley National Laboratory.
□ The Molecular Foundry, Lawrence Berkeley National Laboratory.
● Present address: Redwood Bioscience Inc., Berkeley, California 94704.
(1) Akkerman, H. B.; Kronemeijer, A. J.; van Hal, P. A.; de Leeuw, D. M.; Blom, P. W.; de Boer, B. *Small* **2008**, *4*, 100–104.
(2) Sam, M.; Boon, E. M.; Barton, J. K.; Hill, M. G.; Spain, E. M. *Langmuir* **2001**, *17*, 5727–5730.
(3) Godula, K.; Rabuka, D.; Nam, K. T.; Bertozzi, C. R. *Angew. Chem., Int. Ed.* **2009**, *48*, 4973–4976.
(4) Choudhuri, K.; Wiseman, D.; Brown, M. H.; Gould, K.; van der Merwe, P. A. *Nature* **2005**, *436*, 578–582.
(5) Parthasarathy, R.; Rabuka, D.; Bertozzi, C. R.; Groves, J. T. *J. Phys. Chem. B* **2007**, *111*, 12133–12135.
(6) Richter, R. P.; Hock, K. K.; Burkhartsmeyer, J.; Boehm, H.; Bingen, P.; Wang, G.; Steinmetz, N. F.; Evans, D. J.; Spatz, J. P. *J. Am. Chem. Soc.* **2007**, *129*, 5306–5307.
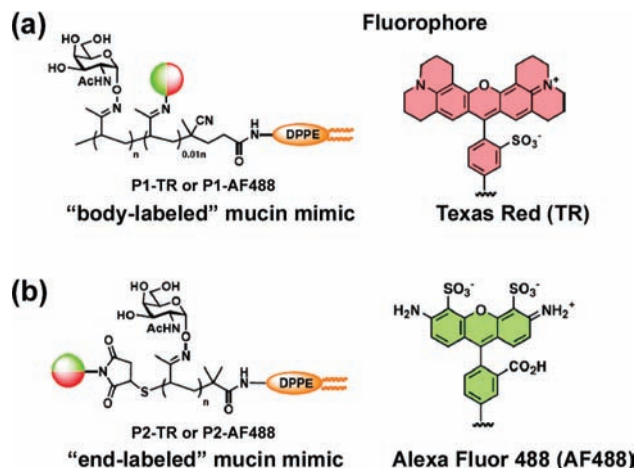(7) Mitra, A. K.; Celia, H.; Ren, G.; Luz, J. G.; Wilson, I. A.; Teyton, L. *Curr. Biol.* **2004**, *14*, 718–724.

Figure 1. Representations of two distinct types of phospholipid-terminated mucin glycoprotein mimetics: (a) "body-labeled" mucin mimic with a small number (2–3) of fluorophores distributed along the glycopolymer backbone ($n \approx 240$), and (b) "end-labeled" mimics containing only one terminal fluorescent dye per polymer chain (green = Alexa Fluor 488, red = Texas Red).

synthetically tractable mucin glycoprotein mimetics and have studied their orientation at cell-free lipid membranes with nanometer precision using interferometric imaging.

Mucins are characterized by a long, rodlike architecture resulting from dense glycosylation of serine and threonine amino acid residues abundantly distributed throughout the peptide backbone.[8] While structurally diverse, mucin carbohydrate epitopes are typically attached to the protein via an α-*O*-linked core sugar, *N*-acetylgalactosamine (GalNAc). In our earlier work,[11] we demonstrated that these native structures can be recreated in synthetic polymers by the attachment of α-aminooxy GalNAc monosaccharides to a methylvinyl ketone (MVK) polymer via stable oxime linkages (Polymer **P1** in Figure 1a). In addition, the glycopolymers were furnished with a small fraction (1% of monomeric units) of Texas Red (TR) fluorophores distributed along the polymer backbone for fluorescence imaging and a terminal phospholipid tail for anchoring in supported lipid bilayers (SLBs). These rodlike mucin mimics (which we refer to as "body-labeled" to characterize the fluorophore distribution) incorporated into two-dimensionally fluid, solid-supported lipid membranes and bound soluble glycan-specific lectin proteins with the same specificities as natural mucins.[11] Interferometric measurements using the intrinsic fluorophores showed a supine orientation, with a mean fluorophore height roughly 1 nm above the membrane.[5]

We have now expanded the structural repertoire of mucin mimetic polymers, focusing especially on modifications that direct the position and type of the polymer's fluorescent probe. Figure 1b depicts a second-generation mucin mimetic architecture (Polymer **P2**), which addresses several key issues associated with our earlier design. Namely, we determined that these glycopolymers would be of narrow chain-length distributions and would feature a GalNAc-decorated poly(MVK) backbone bracketed by a lipid anchor and a single fluorescent probe at opposite ends.

In this paper, we describe the synthesis of these new molecules and their characterization at solid-supported lipid bilayers, made possible by the lipid anchor. Supported bilayers are well-established experimental models of cell membrane architecture that replicate the two-dimensional fluidity and structure of natural membranes while allowing compositional control and a variety of imaging modes.[12–17] The bilayers are supported by reflective silicon substrates with microfabricated silica terraces that make possible the use of fluorescence interference contrast microscopy (FLIC), a technique in which interference between direct and reflected paths of fluorescence light lead to height-dependent fluorescence intensity.[18–22] Analysis of the detected intensities, accounting for the fluorophore spectra and optical setup, reveals the mean fluorophore height within a few nanometers precision.

The mucin mimetic polymers were designed to enable and exploit the topographic power of FLIC imaging. First, the precise end-localization of the fluorescent probe in molecules **P2** dictates that the height determined by FLIC is the height of the molecule, rather than being the average of signals from fluorophores randomly distributed along the body of the polymer, as in **P1**. Second, we created polymers with different fluorescent probes, Texas Red and Alexa Fluor 488 (AF488). Simple lipids are available with conjugated Texas Red and fluorescein (FITC); the FITC excitation and emission spectra are nearly identical to those of Alexa Fluor 488. Comparison of the FLIC signal of mucin glycopolymers and lipids in separate experiments, both with the same or similar fluorescent probe, therefore provides a topographic measure that is robust with respect to potential systematic uncertainties, enhancing the already considerable appeal of FLIC.

Most importantly, comparison of differently labeled polymers, both **P1** and **P2**, allows discrimination of the optical reporter's effect on molecular orientation. We find that Texas Red-labeled molecules are supine, while Alexa Fluor 488-labeled molecules project away from lipid membranes, a profound difference that is striking in light of the small size of the fluorophore relative to that of the whole polymer. These experiments show that macromolecular orientation at membranes (i.e., supine or upright) can be dictated by synthetic design and controlled by small modifications of chemical structure.

Results

Modular Synthesis of Dual End-Functionalized Mucin Mimetic Polymers. The synthesis of TR and AF488-containing "end-labeled" mucin mimics **P2** is shown in Scheme 1, with details provided in the Experimental Methods section. First, we prepared a poly(MVK) intermediate **P3** of narrow chain length distributions using reversible addition–fragmentation chain

(8) Strous, G. J.; Dekker, J. *Crit. Rev. Biochem. Mol. Biol.* **1992**, *27*, 57–92.
(9) Theodoropoulos, G.; Carraway, K. L. *J. Cell. Biochem.* **2007**, *102*, 1103–1116.
(10) Gendler, S. J. *J. Mammary Gland Biol. Neoplasia* **2001**, *6*, 339–353.
(11) Rabuka, D.; Parthasarathy, R.; Lee, G. S.; Chen, X.; Groves, J. T.; Bertozzi, C. R. *J. Am. Chem. Soc.* **2007**, *129*, 5462–5471.

(12) Boxer, S. G. *Curr. Opin. Chem. Biol.* **2000**, *4*, 704–709.
(13) Castellana, E. T.; Cremer, P. S. *Surf. Sci. Rep.* **2006**, *61*, 429–444.
(14) Groves, J. T.; Boxer, S. G. *Acc. Chem. Res.* **2002**, *35*, 149–157.
(15) Tamm, L. K.; McConnell, H. M. *Biophys. J.* **1985**, *47*, 105–113.
(16) Harland, C. W.; Rabuka, D.; Bertozzi, C. R.; Parthasarathy, R. *Biophys. J.* **2008**, *94*, 4718–4724.
(17) von Tscharner, V.; McConnell, H. M. *Biophys. J.* **1981**, *36*, 421–427.
(18) Lambacher, A.; Fromherz, P. *J. Opt. Soc. Am. B* **2002**, *19*, 1435–1453.
(19) Kiessling, V.; Tamm, L. K. *Biophys. J.* **2003**, *84*, 408–418.
(20) Groves, J. T.; Parthasarathy, R.; Forstner, M. B. *Annu. Rev. Biomed. Eng.* **2008**, *10*, 311–338.
(21) Parthasarathy, R.; Groves, J. T. *Proc. Natl. Acad. Sci. U.S.A.* **2004**, *101*, 12798–12803.
(22) Ajo-Franklin, C. M.; Yoshina-Ishii, C.; Boxer, S. G. *Langmuir* **2005**, *21*, 4976–4983.

Scheme 1. Synthesis of "End-Labeled" Mucin Mimics

ACVA = 4,4'-azobis(4-cyanovaleric acid, DPPE = 1,2-dipalmitoyl-*rac*-glycero-3-phosphoethanolamine

transfer (RAFT) polymerization.[23,24] Polymerization of MVK (**1**) in the presence of a radical initiator and the phospholipid-containing trithiocarbonate chain transfer agent **2**, a chain-growth mediator, allowed us to simultaneously control the polydispersity (PDI = 1.10) of the resulting polymer and to introduce an SLB anchor and a point of fluorophore attachment at each terminus of the resulting polymer chains. Condensation of intermediate **P3** with α-aminooxy GalNAc furnished glycopolymer **P4** with a terminal lipid tail and pendant mucin-like glycans. The free terminal sulfhydryl group released under the condensation conditions was capped with a maleimide-conjugated TR or AF488 fluorophore, thus, completing the assembly of the target fluorescent mucin mimics **P2**. The efficiency of glycan ligation was established by NMR analysis to be approximately 60%, which was in good agreement with the previously synthesized "body-labeled" mucin mimic **P1**.[11]

The **P2** polymers adopted extended mucin-like conformations with lengths of approximately 30 nm, as determined by several methods. The hydrodynamic radii of polymers **P2-TR** and **P2-AF488** were 31 ± 7 and 25 ± 5 nm, respectively, obtained by dynamic light scattering (DLS) in PBS buffer (pH = 7.2). More direct evidence of their extended form was obtained by TEM imaging of single glycopolymer chains (Figure 2). Theoretical length values calculated for fully extended 240-monomer unit polymers **P2** using MM2 force field-based molecular mechanics predictions were approximately 35 nm, consistent with the experimental measures. As reported previously, polymers **P1** with similar degree of polymerization also adopted extended conformations approximately 30 nm long.[5]

Insertion of Lipid-Terminated Mucin Mimics into Supported Lipid Bilayers and Their Analysis by FRAP. The lipid tail of the mucin glycopolymers allowed for their integration with solid-supported lipid membranes. Molecules **P2-TR** and **P2-AF488** incorporated into supported lipid bilayers are illustrated schematically in Figure 3a. The bilayer preparation and polymer incubation are as described earlier[5] and are also detailed in the Experimental Methods section. In all experiments, the use of a small fraction of fluorophore-conjugated lipids,

spectrally distinct from the probes conjugated to the polymers, allowed independent examination of the bilayer and the glycopolymers.

Fluorescence imaging of the glycopolymers indicated robust membrane incorporation. Absolute quantification of molecular density from fluorescence brightness is, in general, challenging.[25] Comparison of the brightness of the membrane-incorporated Texas Red-labeled polymer **P2-TR** with membranes containing controlled fractions of Texas Red conjugated lipids allows determination of the surface density of molecule **P2-TR**, found to be approximately 20,000 molecules/μm^2. No Alexa Fluor 488-labeled lipids are available, prohibiting a similar quantification of density for molecule **P2-AF488**. However, as its structure is nearly identical to that of molecule **P2-TR**, featuring the same lipid anchor, its density is likely to be similar.

Lateral mobility is an important attribute of membrane-incorporated molecules. FRAP measurements,[11] as illustrated in Figure 3b, showed the glycopolymers to be two dimensionally fluid with diffusion coefficients D of 1.7 ± 0.7 μm^2/s and 0.9 ± 0.2 μm^2/s for polymers **P2-AF488** and **P2-TR**, respectively. These mobilities are similar to those of the membrane lipids, D = 1.2 ± 0.4 μm^2/s, consistent with anchoring of the polymers in the membrane via their lipid tails. We discuss the difference

(23) Chiefari, J.; Chong, Y. K.; Ercole, F.; Krstina, J.; Jeffery, J.; Le, T. P. T.; Mayadunne, R. T. A.; Meijs, G. F.; Moad, C. L.; Moad, G.; Rizzardo, E.; Thang, S. H. *Macromolecules* **1998**, *31*, 5559–5562.
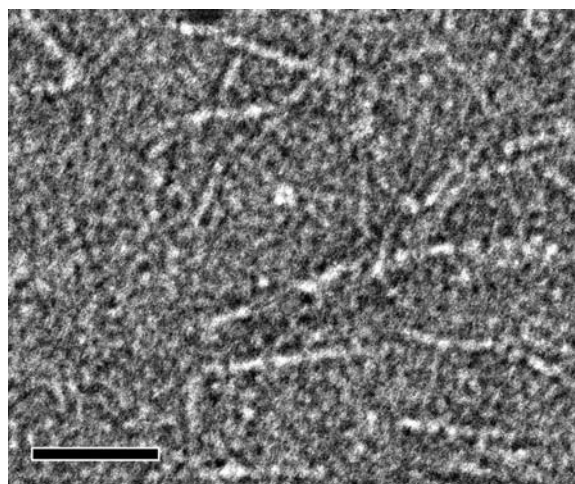(24) Cheng, C.; Sun, G.; Khoshdel, E.; Wooley, K. L. *J. Am. Chem. Soc.* **2007**, *129*, 10086–10087.
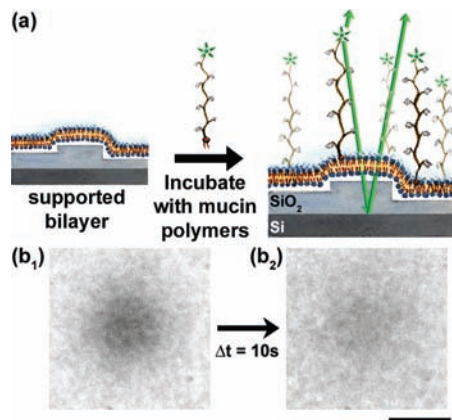
Figure 2. Transmission electron micrograph of polymers **P2-AF488** showing rodlike extended molecular conformations. Bar = 50 nm.

Figure 3. (a) Schematic illustration of polymer incorporation in a supported lipid bilayer and FLIC imaging using end-labeled fluorophores. Optical interference between direct and reflected optical paths leads to height-dependent fluorescence intensity. A terraced oxide layer on the reflective substrate enables parallel measurements with different path length differences and hence greater precision in determining the mean fluorophore height. The illustration is not to scale. (b) Fluorescence images of **P2-AF488** incorporated into a supported lipid bilayer. Bar = 15 μm. Fluorescence recovery after photobleaching (FRAP) demonstrates the fluidity of the membrane-anchored mucin mimics. (b_1) Fluorophores labeling the polymer were bleached in the central zone; (b_2) the same field of view after 10 s.

Figure 4. (a) and (b) Fluorescence images of labeled polymers and lipids at a membrane supported by a terraced SiO_2/Si substrate. Both depict the same region on the same substrate. Bar = 50 μm. (a) Fluorescence image of **P2-AF488**, polymers labeled at the distal end with Alexa Fluor 488. (b) Fluorescence image of Texas Red-labeled lipids. (c) and (d) Fluorescence intensity versus SiO_2 terrace height for the data of images (a) and (b), respectively. Circles indicate the measured intensities. The fitted curves yield the mean fluorophore height, $z = 17 \pm 6$ nm and $z = 4 \pm 4$ nm for (c) and (d), the polymer and the lipid, respectively.

Table 1. FLIC-Derived Height Measurements for Mucin Mimetic Glycopolymers at Supported Lipid Bilayers

polymer (label)	polymer z (nm)	lipid z (nm)	Δz (nm)
P2-AF488	16.7 ± 1.0	5.5 ± 0.4	11.2 ± 1.1
P2-TR	5.4 ± 2.3	5.1 ± 2.1	0.2 ± 2.0
P1-AF488	14.4 ± 1.2	5.8 ± 0.9	8.6 ± 1.2
P1-TR	5.3 ± 1.0	4.4 ± 1.6	0.9 ± 1.8

between the D values of **P2-AF488** and **P2-TR** below. The lipidlike mobility and the laterally homogeneous fluorescence images imply that the glycopolymers do not aggregate.

Determination of the Orientation of Membrane-Bound Mucin Mimics by FLIC Imaging. To probe the orientation of the membrane-incorporated polymers, we used Fluorescence Interference Contrast Microscopy (FLIC), *vide supra*. The raw data consist of fluorescence images of the labeled molecules of interest, lipids or polymers, on reflective substrates with terraced oxide layers (Figure 3a). These provide the intensity as a function of the terrace thickness, data that are then fit to a functional form that reveals the mean height of the probe above the oxide. We show in Figure 4a a representative fluorescence image from a sample with membrane-incorporated molecule **P2-AF488**, the mucin mimetic glycopolymer with AlexaFluor 488 at the distal end. The intensity and terrace height values are plotted in Figure 4c, with a fit that yields a mean fluorophore height of $z_{\text{P2-AF488}} = 17 \pm 6$ nm above the oxide surface. In Figure 4b, we show the fluorescence from Texas Red-labeled lipids from the *same* membrane, with the corresponding data and fit (Figure 4d): $z_{\text{lipid}} = 4 \pm 4$ nm. The data from several samples ($N = 13$) reveal a polymer probe height $z_{\text{P2-AF488}} = 16.7 \pm 1.0$ nm, a lipid probe height $z_{\text{lipid}} = 5.5 \pm 0.4$ nm, and a difference between the two, $\Delta z_{\text{P2-AF488}} = z_{\text{P2-AF488}} - z_{\text{lipid}} = 11.2 \pm 1.1$ nm. These values are also provided in Table 1. The FLIC data reveal that the Alexa Fluor 488-labeled polymers **P2-TR** project out from the membrane.

Effects of Physical and Electrostatic Properties of the Terminal Label on Macromolecular Orientation. Markedly different behavior is exhibited by molecule **P2-TR**, the mucin mimetic glycopolymer with Texas Red at the distal end, incorporated at supported lipid bilayers. For these, FLIC imaging reveals Texas Red probe heights $z_{\text{P2-TR}} = 5.4 \pm 2.3$ nm for the glycopolymer, $z_{\text{lipid}} = 5.1 \pm 2.1$ nm for FITC-labeled lipids from the same membranes, and a difference
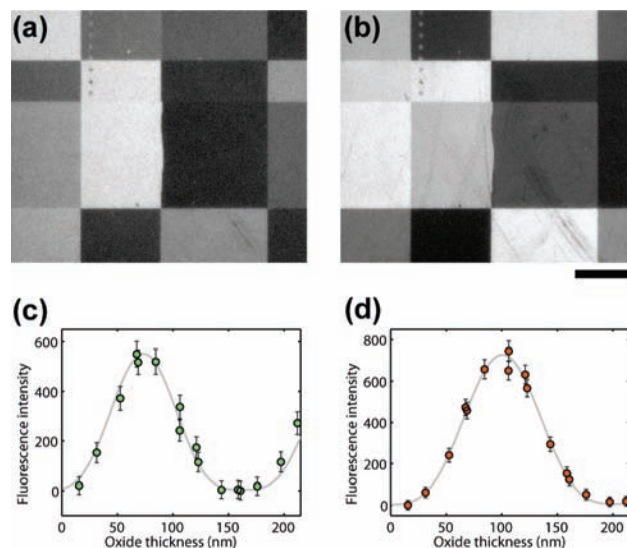
(25) Galush, W. J.; Nye, J. A.; Groves, J. T. *Biophys. J.* **2008**, *95*, 2512–2519.

between the two $\Delta z_{\text{P2-TR}} = 0.2 \pm 2.0$ nm ($N = 17$); see also Table 1. The FLIC data reveal that the Texas Red-labeled polymers **P2-TR**, identical to **P2-AF488** except for the fluorescent probe, lie flat at the membrane.

Effects of Fluorophore Positioning within the Macromolecule on the Outcome of FLIC Analysis. We also examined SLB-incorporated polymer **P1-AF488**, labeled with Alexa Fluor 488 along the MVK backbone, which showed a polymer probe height $z_{\text{P1-AF488}} = 14.4 \pm 1.2$ nm. The Texas Red lipid probe height was $z_{\text{lipid}} = 5.8 \pm 0.9$ nm; the difference between the two, $\Delta z_{\text{P1-AF488}} = z_{\text{P1-AF488}} - z_{\text{lipid}} = 8.6 \pm 1.2$ nm ($N = 9$). Polymer **P1-TR**, identical except for labeling with Texas Red rather than Alexa Fluor 488, was examined in earlier work:[5] $z_{\text{P1-TR}} = 5.3 \pm 1.0$ nm, $z_{\text{lipid}} = 4.4 \pm 1.6$ nm, and $\Delta z_{\text{P1-TR}} = 0.9 \pm 1.8$ nm. (In these experiments, z_{lipid} was measured using Texas Red-labeled lipids in different membrane samples, so the stated $\Delta z_{\text{P1-TR}}$ is the difference of the average $z_{\text{P1-TR}}$ and z_{lipid}, rather than the average of the differences for each sample as in the measurements of **P2-TR**, **P2-AF488**, and **P1-AF488**).

Effects of Ionic Strength of the Aqueous Environment on Mucin Mimic Orientation. Experiments conducted in deionized water (ionic strength ≈ 10 μM) and in phosphate buffered saline (PBS, pH = 7.4, ionic strength 150 mM) yielded statistically identical topographic data. For **P2-AF488** at lipid bilayers, $\Delta z_{\text{P2-AF488}} = 11.4 \pm 1.3$ nm in deionized water and $\Delta z_{\text{P2-AF488}} = 11.0$

± 1.1 nm in PBS. For **P2-TR**, $\Delta z_{P2\text{-}TR} = 0.1 \pm 2.5$ nm in deionized water and $\Delta z_{P2\text{-}TR} = 0.4 \pm 2.4$ nm in PBS.

Discussion

Fluorescence imaging and mobility measurements reveal membrane-incorporation of the lipid-terminated mucin mimetic glycopolymers. Structural data demonstrate the expected extended rodlike structure of the polymers. FLIC imaging reveals the orientation of the molecules at solid-supported membranes, i.e. whether they project out from the membrane or lie flat.

FLIC imaging provides topographic information about macromolecules at the nanometer scale, a regime that is difficult to probe with other techniques. For instance, the diffraction limit of conventional optics renders simple microscopy inadequate. Electron microscopy is susceptible to experimental artifacts and uncertainties due to the requisite staining and immobilization of samples. Atomic force microscopy is slow and can be complicated by pernicious tip–sample interactions. FLIC, in contrast, is rapid, precise, and noninvasive, enabling standard fluorescent probes to convey information about molecular conformation and orientation.

Strikingly, we find that polymers labeled with Alexa Fluor 488 project out from the membrane surface, whereas otherwise identical Texas Red-labeled polymers are topographically indistinguishable from membrane lipids. The fluorescent probes are structurally a minor component of the molecules, contributing only about 2% of the molecular weight. Texas Red, however, is known to insert into lipid bilayers,[20,26] and the molecular underpinnings of its hydrophobicity have recently been illuminated.[27] Despite the hydrophilic nature of the rest of the polymer, the fluorophore's hydrophobicity appears sufficient to anchor the polymer's distal end to the membrane. Double-anchoring of the Texas Red-labeled molecule **P2-TR**, mediated by both its lipid anchor and by the Texas Red fluorophore, is the likely cause of the 2-fold lower diffusion coefficient of **P2-TR** compared to that of **P2-AF488** in membranes. Alexa Fluor 488 contains multiple negative charges, rendering the fluorophore hydrophilic.

These polymers are uncharged and, as expected, show no detectable ionic-strength dependence in their orientation. Their orientation should therefore be largely determined by entropic concerns, with projection from the membrane maximizing the volume available to rodlike membrane-anchored macromolecules. A rod of length L anchored at a point, freely exploring a hemisphere of allowed orientations, has a mean surface-to-end height $L/2$. The expected height above the membrane, Δz, for polymers **P2**, for which $L \approx 30$ nm, should therefore be approximately 15 nm, consistent with the $\Delta z_{P2\text{-}AF488} = 11.2 \pm 1.1$ nm value observed for the Alexa Fluor 488-labeled polymer.

The measured surface density of approximately 20,000 **P2** molecules/μm^2 corresponds to a mean intermolecular spacing of roughly 8 nm, assuming 6-fold liquidlike coordination. This is greater than the width of the rodlike polymers of approximately 2 nm, again supporting the conclusion that orientational entropy, rather than dense packing, controls the **P2-AF488** orientation.

Our observation that fluorophore type dramatically influences molecular orientation is not only important to the present case of membrane-bound mucin mimetic polymers but is also generally of more consequence to the fields of chemistry, biology, and biophysics. Ubiquitous fluorescent probes are not necessarily inert readouts of molecular properties but can cause significant physical perturbations. More positively, our findings imply that control of molecular orientation, not only at membranes but also in, for example, molecular electronics and nucleic acid arrays, can be afforded by small modifications of molecular structure. Technical extensions of FLIC to probe the orientation of single molecules, though technically challenging, may offer still deeper insights into possible topographic heterogeneity of a population.

Experimental Methods

General Methods. All chemicals, unless stated otherwise, were purchased from Aldrich Chemicals. Texas Red (TR) and Alex Fluor 488 (AF488) maleimide conjugate were purchased from Invitrogen. Solvents were purified on a Glass Contour solvent purification system. Nuclear magnetic resonance (NMR) spectra were recorded on Bruker Biospin Advance II 500 MHz high performance NMR spectrometer with multinuclear CP-MAS probe. Spectra were recorded in CDCl$_3$ or D$_2$O solutions at 293 K and referenced to residual solvent peaks. Infrared spectra were collected on a Varian 3100 FT-IR spectrometer. ATR analyses were performed using Pike Technologies MIRacle single refraction ATR accessory (ZnSe crystal). Size exclusion chromatography (SEC) was performed on a Viscotek TDA 302 SEC system with triple detector array. For measurements in DMF (0.2% LiBr) the instrument was equipped with two in-series Mixed Bed GMHHR-M columns, separation range 100–4 M (30 cm × 7.8 mm i.d.) at 70 °C. Transmission electron microscopy was performed on a Jeol 2100F transmission electron microscope operated at 200 kV.

Glycopolymer Synthesis. Synthesis of the Chain Transfer Agent (2). A pressure-seal tube (25 mL) equipped with a magnetic stirring bar was charged with S-dodecyl-S'-(α,α-dimethylpentafluorophenyl acetate)trithiocarbonate[3] (365 mg, 0.69 mmol) and 1,2-dipalmitoyl-*rac*-glycero-3-phosphoethanolamine (476 mg, 0.69 mmol) under a stream of nitrogen. Mixture of chloroform and methanol (20:1, 7 mL) was added, followed by diisopropylethylamine (600 μL, 3.44 mmol, 5 equiv). The headspace was filled with nitrogen, and the tube was sealed. The content was heated at 65 °C for 5 h. After this time, the solvents were removed, and the residue was chromatographed (silica gel, 5% → 10% methanol/chloroform with 1% acetic acid) to give yellow solid (507 mg, 71%). ^{1}H NMR (CDCl$_3$, 500 MHz) δ: 5.28 (bm, 1H), 4.39 (bm, 1H), 4.18 (bm, 1H), 3.97–3.90 (bm, 4H), 3.48 (bm, 1H), 3.27 (t, J = 7.0 Hz, 2H), 2.46–1.95 (bm, 8H), 1.75–1.50 (bm, 12H), 1.45–1.15 (m, 62H), 0.89 (m, 9H). ^{13}C NMR (CDCl$_3$, 125 MHz) δ: 220.3, 173.6, 173.4, 70.4, 63.7, 57.2, 40.9, 37.1, 34.3, 34.1, 31.9, 29.8, 29.7, 29.6, 29.5, 29.5, 29.4, 29.3, 29.2, 29.1, 27.7, 25.6, 25.0, 24.9, 22.7, 14.1. FT-IR (KBr, CH$_2$Cl$_2$) ν (cm^{-1}): 3372, 2920, 2851, 1742, 1661, 1530, 1468, 1242, 1074, 816. HRMS (*m/z*): 1038.6684 (calculated), 1038.6677 (found).

Synthesis of Lipid-Terminated MVK Polymer P3. A flame-dried Schlenk flask (10 mL) equipped with a magnetic stirring bar was charged with **2** (21.3 mg, 0.021 mmol, 0.50 mol %), ACVA (4,4′-azobis(4-cyanovaleric acid), 1.1 mg, 0.004 mmol, 0.10 mol %), methylvinylketone (287.5 mg, 4.102 mmol, freshly distilled and filtered through basic alumina) and 2-butanone (377 mg, freshly distilled and filtered through basic alumina). The flask was equipped with a rubber septum and attached to a Schlenk line. The yellow solution (43 wt % in monomer) was thoroughly degassed by three freeze–pump–thaw cycles. After the final cycle, the flask was allowed to warm to room temperature and then immersed into an oil bath preheated to 65 °C. After 16 h, the reaction mixture was diluted with CH$_2$Cl$_2$ and precipitated into hexanes. The residue was redissolved in a minimal quantity of CH$_2$Cl$_2$ and precipitated again into hexanes with vigorous stirring. This was repeated twice more. The yellow polymer was concentrated in vacuo from CH$_2$Cl$_2$ three

(26) Baumgart, T.; Hunt, G.; Farkas, E. R.; Webb, W. W.; Feigenson, G. W. *Biochim. Biophys. Acta - Biomembranes* **2007**, *1768*, 2182–2194.
(27) Skaug, M. J.; Longo, M. L.; Faller, R. *J. Phys. Chem. B* **2009**, *113*, 8758–8766.

times to remove residual hexanes and dried under high vacuum overnight to give polymer **P2** as a pale-yellow solid (253 mg, 82%). SEC (DMF, 2% LiBr): M_w = 17.5 kDa, M_n = 15.9 kDa, DP ≈ 240, PDI = 1.10. ^{1}H NMR (CDCl$_3$, 500 MHz) δ: 5.28−4.90 (bm, 2H), 4.45 (bm, 1H), 4.18 (bm, 1H), 4.20−3.69 (bm, 3H), 3.38 (bm, 2H), 3.21 (bm, 1H), 2.65−2.10 (bm, 716H), 2.00 −1.85 (bm, 88H), 1.85−1.40 (m, 221H), 1.35−1.00 (bm, 155H), 0.89 (m, 9H). FT-IR (KBr, CH$_2$Cl$_2$) ν (cm^{-1}): 3406, 2926, 2854, 1710, 1427, 1356, 1242, 1165, 961, 735.

Synthesis of Glycopolymer P4. A vial (4 mL) equipped with a magnetic stirring bar was charged with alkyne-terminated polymer **P3** (4.0 mg, 57.1 μmol of keto-groups) and α-aminooxy-GalNAc (14 mg, 59.3 μmol, 1.03 equiv). THF (0.2 mL) was added, and the polymer was allowed to dissolve; then 50 mM sodium phosphate buffer (0.2 mL, pH = 5.2) was added. The headspace was filled with nitrogen; the vial was capped and heated at 50 °C for 20 h. After this time, the solvents were removed, and the crude product was dialyzed against distilled water for 24 h with the water being changed periodically. The product was lyophilized to yield a fluffy, white solid (8.4 mg, 80%). Estimated from ^{1}H NMR: 56% GalNAc incorporation, M_w = 45.2 kDa, DP ≈ 240. ^{1}H NMR (D$_2$O, 500 MHz) δ: 5.50−5.35 (bm, 1H), 4.35−3.40 (bm, 6H), 2.90−0.50 (bm, 13.6H).

Synthesis of Alexa Fluor 488-Conjugated Glycopolymer P2-AF488. In a vial (4 mL) polymer **P4** (4.3 mg, 0.91 × 10^{-4} mmol of thiol groups) was dissolved in TRIS buffer (0.50 mL, 50 mM, pH = 8) containing Alexa Fluor 488-maleimide (0.41 mg, 5.69 × 10^{-4} mmol, 5 equivalents) and TCEP (0.5 mg). The reaction mixture was stirred at ambient temperature for 20 h. After this time, the polymer was purified on a Sephadex G25 column and lyophilized to give an orange solid (3.2 mg, 74%). ^{1}H NMR (D$_2$O, 500 MHz) δ: 5.60−5.15 (bm, 1H), 4.40−3.50 (bm, 6H), 2.55−0.40 (bm, 13H). ATR (ZnSe) ν (cm^{-1}): 3304, 2912, 1638, 1553, 1450, 1368, 1117, 1047, 868.

Synthesis of Texas Red-Conjugated Glycopolymer P2-TR. This polymer was prepared using a procedure identical to that for **P2-AF488**, with the following exceptions: polymer **P4** (3.4 mg, 1.15 × 10^{-4} mmol of thiol groups) was dissolved in TRIS buffer (0.50 mL, 50 mM, pH = 8) containing Texas Red-maleimide (0.33 mg, 4.55 × 10^{-4} mmol, 5 equiv) and TCEP (0.5 mg). After purification by Sephadex G25 column, **P2-TR** was isolated as a purple solid (2.4 mg, 71%). ^{1}H NMR (D$_2$O, 500 MHz) δ: 5.55−5.10 (bm, 1H), 4.35−3.40 (bm, 6H), 2.60−0.50 (bm, 13H). ATR (ZnSe) ν (cm^{-1}): 3316, 2918, 2848, 1647, 1554, 1375, 1117, 1051, 918.

Polymer **P1-AF488** was prepared in a fashion identical to that described previously,[11] and its ^{1}H NMR spectrum is available in the Supporting Information.

Note: The lipid-terminated glycopolymers displayed aggregation behavior in aqueous solutions at the minimal concentrations suitable for analysis by size exclusion chromatography. This behavior precluded us from determining their polydispersities using this technique.

Transmission Electron Microscopy (TEM). Polymers were deposited on a carbon grid from a solution (0.1 mg/mL) in 0.1 M PBS buffer (0.15 M NaCl, pH = 7.2) over 30 min. The grid was stained with 1% solution of phosphotungstic acid (PTA) for 20 min, necessary for obtaining reasonable contrast, washed, dried, and imaged.

Molecular Models. Molecular models were constructed using the MM2 energy minimization algorithm in CS Chem 3D Pro.

Lipid Membranes. SLBs were formed by standard vesicle fusion techniques.[12] The bilayers in which **P2-AF488** was integrated were composed of 99.5 mol % DOPC (1,2-dioleoyl-*sn*-glycero-3-phosphocholine, purchased from Avanti Polar Lipids), a zwitterionic

lipid, and 0.5 mol % Texas Red DHPE (Texas Red 1,2-dihexade-canoyl-*sn*-glycero-3-phosphoethanolamine, purchased from Invitrogen), a fluorescent lipid probe. The bilayers in which **P2-TR** was integrated were composed of 97 mol % DOPC and 3 mol % FITC DHPE (*N*-(fluorescein-5-thiocarbamoyl)-1,2-dihexadecanoyl-*sn*-glycero-3-phosphoethanolamine, purchased from Invitrogen), a fluorescent lipid probe. As in our earlier work,[5] following its assembly, the bilayer is incubated with the mucin mimetic polymers (∼20 μg/mL, 15 h), unbound polymer is washed away, and the resulting membrane is imaged by epifluorescence microscopy using a Nikon TE2000 inverted fluorescence microscope and a Hamamatsu ORCA CCD camera. Molecular mobilities of lipids and polymers were measured by fluorescence recovery after photobleaching (FRAP), performed and analyzed as in ref 11.

Terraced Substrates and FLIC Analysis. We employed FLIC imaging to study the orientation of the membrane-anchored mucin mimetic polymers.[5] The membranes are assembled on SiO$_2$ on a reflective silicon substrate. Interference of the fluorescence excitation light, as well as the emitted light, with its reflection from the substrate leads to height-dependent fluorescence intensity (Figure 2a). Accounting for the optical parameters of the setup, one can extract topographic information from the fluorescence intensity data. We use the same approach as in ref 5. FLIC image analysis is described in detail in ref 20. Providing multiple SiO$_2$ terraces of known thickness and measuring the fluorescence intensity as a function of terrace height reveals the height of the fluorophores above the oxide within a few nanometers precision. Using standard lithographic techniques, we microfabricated SiO$_2$/Si substrates with arrays of 16 oxide terraces with thicknesses distributed between 0 and 225 nm.[20] FLIC data consisted of background-subtracted fluorescence intensities of the fluorophores of interest on oxide terraces of various (measured) thicknesses. Using software we have developed that calculates theoretical FLIC response functions and compares these to the experimentally derived intensities, we determined for each sample the fluorophore height that best-fit the data with no free parameters other than an overall (irrelevant) fluorescence brightness value. The uncertainties stated in the text are the standard deviations over several samples, the number being stated in the text.

Supporting Information Available: Spectral data for compound **2**, polymers **P2**−**P4** and **P1-AF488**, as well as additional TEM images of **P2-AF488**. This material is available free of charge via the Internet at http://pubs.acs.org.

JA903114G